Electronic Structures of Graphene/MoS_2 Heterostructure: Effects of Stacking Orientation, Element Substitution, and Interlayer Distance

Dian Putri Hastuti[1*], Kenji Nawa[1,2], and Kohji Nakamura[1]

[1]*Graduate School of Engineering, Mie University, 1577 Kurimamachiya-cho, Tsu city, Mie 514-8507, Japan*

[2]*Research Center for Magnetic and Spintronic Materials, National Institute for Materials Science, 1-2-1 Sengen, Tsukuba, Ibaraki 305-0047, Japan*

Corresponding author:

tel: +81-8065026351
email: 420DE01@m.mie-u.ac.jp

Received: June 17, 2022
Accepted: October 20, 2022

DOI: 10.22146/ijc.75538

Abstract: *Effects of stacking orientation, element substitution, and interlayer distance on electronic structures of graphene/MoS_2 heterostructures were investigated using first-principles calculations. The results predicted that the stacking orientation does not take a crucial role in changing the electronic structures in contrast to element substitution, which converts the system from semiconductor to metallic. A bandgap opening originating in a Dirac band of graphene is found to be governed by the interface distance between graphene and MoS_2 layers.*

Keywords: *graphene; transition-metal dichalcogenide; heterostructure; electronic structure; first-principles calculations*

■ INTRODUCTION

Graphene, a stable two-dimensional (2D) material with a honeycomb structure [1-2], has attracted significant attention both in experimental and theoretical studies for decades [3]. Graphene has excellent properties in ultra-high intrinsic mobility and large electrical conductivity [4], making graphene have many potential applications in electronic devices, transparent electrodes, and spintronics devices [1,5]. The low intrinsic spin-orbit coupling (SOC) strength in graphene further provides an advantage in spin transports [6]. However, the absence of bandgap in graphene limits graphene usage in electronics due to its poor on/off ratio [7]. Although many efforts on the bandgap opening have been carried out previously in various ways, such as doping [8-10], creating multilayer graphene [11], and constructing bilayer graphene that demonstrates an electrically gate-controlled, continuously tunable bandgap of up to 250 meV [12], applying an electric field [5], and forming heterostructures [7,13-16], the understanding of the electronic structure of graphene, e.g., focusing the bandgap opening, is crucial for making graphene applicable in a broader area.

Transition-metal dichalcogenide (TMD) is a desired group of materials due to their outstanding properties in potential utilization, such as for electronic devices, optoelectronic devices [17], gas sensing [18] and energy storage [19]. MoS_2, as a member of TMD, shows intriguing mechanical and electrical properties [20]. Unlike graphene, two-dimensional MoS_2 is an excellent semiconductor with a 1.8 eV bandgap. Meanwhile, the bulk system has a 1.2 eV indirect bandgap [21-22]. It further notes that TMD possesses a strong intrinsic SOC of tens of meV compared to graphene [23]. A direct bandgap in two-dimensional MoS_2 could be a solution for bandgap opening on graphene and become the motivation to combine both materials as a heterostructure.

For years, keen interest has been given to heterostructure materials [15,24-27]. A number of the previous studies show exemplary implementations for a heterostructure of graphene and TMD, for example, graphene/MoS_2, applied to supercapacitors, gas sensors, spintronic devices, and electrochemical detectors of Morin [28-29]. Heterostructures of the others, graphene/$MoSe_2$ and graphene/WTe_2, are potential materials in the optoelectronic field [30-31],

graphene/$MoTe_2$ and graphene/WSe_2 are also beneficial in photodetector devices [32-33], and graphene/WS_2 is a prospective material for nanoelectronics and optoelectronic devices [34-35].

In the present work, we have systematically performed density functional theory (DFT) calculations to clarify the effects of the electronic structure of graphene/MoS_2 on stacking, element substitution, and interlayer distance. We find that stacking orientation is not significantly affecting the electronic structures, which contrasts with how element substitution and interlayer distance successfully tune the electronic structures. The findings are essential to navigating the tuning of electronic properties of graphene/MoS_2 heterostructure since they directly impact practical applications.

■ COMPUTATIONAL DETAILS

First-principles calculations using the full-potential linearized augmented plane-wave (FLAPW) method that treats a single slab geometry [36-37] were carried out to investigate the electronic structures of graphene/MoS_2. Generalized gradient approximation (GGA) was employed as exchange correlation [38] and to account for long-range dispersion correction, and the DFT-D2 method was introduced [39]. The core states were treated fully relativistically, and the valence states were treated semi-relativistically, where spin-orbit coupling was incorporated using the second variational method [40]. The LAPW basis with a cutoff of $|k+G| \leq 5.0$ Bohr-1 and muffin-tin (MT) sphere radii of 2.6 Bohr for Mo, 1.9 Bohr for S, Se, and Te, and 1.2 Bohr for C were used, and lattice harmonics with angular momenta up to $l = 8$ for Mo and S, and 6 for C were employed to expand the charge density, potential, and wavefunctions. A 15×15 k-point mesh was used for self-consistent field (SCF) calculations. Atomic force calculations fully optimized all the heterostructures.

As for models, graphene/MoS_2 heterostructures with two different later-stacking orientations, namely, C_S stacking for C atoms stacked on the top of S atoms and C_{Mo} stacking for C atoms stacked on the top of Mo atoms, as illustrated in Fig. 1. These stacking orientations were considered based on the previous study which analyzed the most stable stacking for bilayer MoS_2 [41]. The structural periodicity in graphene and MoS_2 layers sets with two ratios, 1:1 and 4:3, i.e., the 1:1 heterostructure consists of 1×1 cell of both graphene and MoS_2 while the 4:3 heterostructure is 4×4 of graphene and 3×3 of MoS_2. For the element substitution, then, three graphene/TMD heterostructures, consisting of graphene/MoS_2, graphene/$MoSe_2$, and graphene/$MoTe_2$, respectively, were considered. Finally, the dependence of interlayer distance between graphene and MoS_2 in the heterostructure was analyzed by varying the distance from 2.6 to 3.6 Å.

■ RESULTS AND DISCUSSION

Effect of Stacking Orientation

We first confirmed that the calculated lattice constants of single monolayers of graphene and MoS_2 are 3.16 and 2.46 Å, respectively, which agree with the previous works [42]. Fig. 1 displays the optimized 1:1 and 4:3 heterostructures of graphene/MoS_2 for the C_s and C_{Mo} stackings. In the 1:1 heterostructure, for both C_s and C_{Mo} stackings, the bond lengths of C-C in the graphene layer and Mo-Mo atoms in the MoS_2 layer are 1.73 and 3.09 Å, respectively, and the interlayer distances between graphene and MoS_2 layers are 3.38 Å. Even in the 4:3 heterostructure, the interlayer distances in the C_S

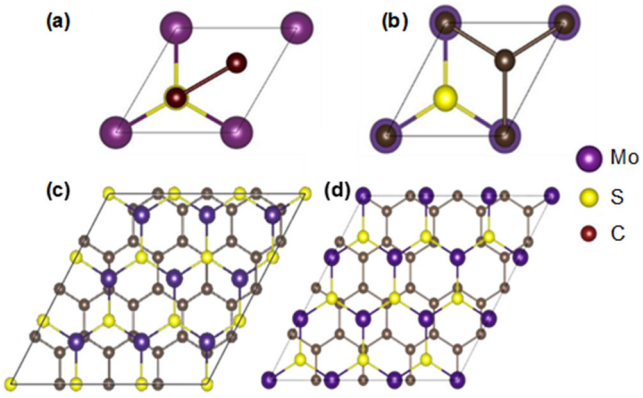

Fig 1. Top view of arrangements of graphene/MoS_2 heterostructure: (a) 1:1 heterostructure with C_S stacking, (b) 1:1 heterostructure with C_{Mo} stacking, (c) 4:3 heterostructure with C_S stacking, and (d) 4:3 heterostructure with C_{Mo} stacking. Purple, yellow, and brown balls represent Mo, S, and C atoms, respectively

and C_{Mo} stackings are 4.47 and 3.50 Å, respectively, and the present results correspond to the previous works [43-44]. Despite the change in the stacking orientations, the structural properties remain the same.

Fig. 2 shows the calculated band structures and densities of states (DOSs) of the 1:1 and 4:3 heterostructures in the C_S and C_{Mo} stackings. The identical feature of the Dirac cone in the band structures and DOSs can be seen in each heterostructure regardless of the stackings. The bandgap at K in both stackings is distinguishable, as shown in the figure, where the bandgaps of the C_S and C_{Mo} stackings are 19 and 8.5 meV. The total energy in the C_{Mo} stacking for the 1:1 heterostructure is slightly lower than that in the C_s one by only 0.872 meV/cell. It occurs in the 4:3 heterostructure, where the total energy of C_{Mo} stacking is lower than that on the C_s by 0.54 meV/cell.

Fig. 3 shows the charge density plot for C_{Mo} and C_S stacking orientation for an optimized 1:1 structure. To identify the presence of charge transfer between layers, we calculated the total charge for each atom for MoS_2 and graphene as a unit cell and the total charge for MoS_2-graphene as a heterostructure and compared the values, which later showed no differences.

The physical origin of the bandgap that emerged in the graphene/MoS_2 is due to the hybridization between the graphene and MoS_2 layers, where weak interaction bonds the layers, proven by no charge transfer between both layers. Thus, the stacking orientation does not affect their electronic structures qualitatively, as both have identical band structure and does not change the character of the material. However, stacking orientation changes the band structure quantitatively as the band gap differs from each other. This result also corresponds to the previous study, which studied the 5:4 and 4:4 heterostructures [45].

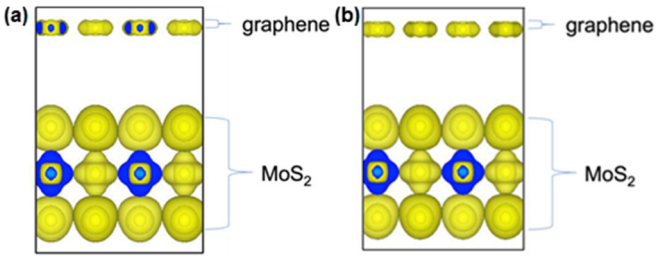

Fig 2. Charge density for optimized 1:1 structure (a) C_{Mo} stacking orientation and (b) C_S stacking orientation. The yellow color shows positive charges

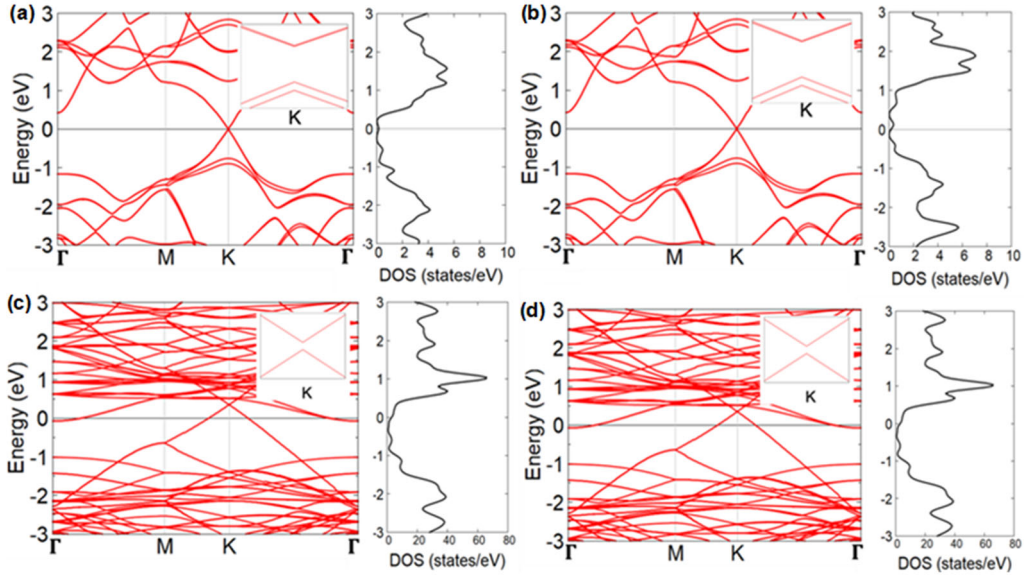

Fig 3. Calculated band structures and DOSs of graphene/MoS_2 heterostructures under different structure arrangements: (a) 1:1 structure with C_S stacking orientation, (b) 1:1 heterostructure with C_{Mo} stacking orientation, (c) 4:3 structure with C_s stacking orientation, and (d) 4:3 structure with C_{Mo} stacking orientation. The insets show a bandgap at K in each structure

Effect of Element Substitution

We next present the results for three different heterostructures, graphene/MoS_2, graphene/$MoSe_2$, and graphene/$MoTe_2$, to examine the effect of element substitution. As for the graphene/MoS_2, we chose the C_{Mo} stacking with the lowest total energy. The calculated interlayer distances and bandgaps for the three heterostructures are given in Table 1, and the band structures are shown in Fig. 4. From the calculated band structures, we observe that the bandgap in the Dirac cone at K of each system variates in nominal values. The graphene/$MoTe_2$ show a metallic characteristic. Enlarged pictures along the G-M-K-G direction show that the Dirac cone for the graphene/$MoTe_2$ is shifting toward the valence bands.

The calculated optimized interlayer distances for the three heterostructures are given in Table 1. The three heterostructures have different values of the optimized interlayer distances, where the graphene/MoS_2 has the most significant distance of 3.38 Å compared to those in the graphene/$MoSe_2$ (3.28 Å) and graphene/$MoTe_2$ (3.19 Å). Alongside the optimized interlayer distance, the calculated bandgaps located on the Dirac cone in graphene are also given in Table 1. Meanwhile, the graphene/MoS_2 has the lowest bandgap of 8.5 meV, while graphene/$MoSe_2$ increases to 15 meV due to the interlayer reduction. For the graphene/$MoTe_2$, where the interlayer distance further decreases, the system becomes metallic, and the energy state of the Dirac cone shifts to 0.8 eV below the Fermi level.

For further analysis, we calculated the projected density of states (PDOS) as shown in Fig. 5. Based on these graphs, we can see that the orbitals which have significant contributions to valence and conduction bands are d orbitals attributed in Mo.

Table 1. Calculated interlayer distance (d) and bandgap (ΔE) of optimized graphene/MoS_2, graphene/$MoSe_2$, and graphene/$MoTe_2$ heterostructure

Elements	d (Å)	ΔE (meV)
graphene/MoS_2	3.38	8.5
graphene/$MoSe_2$	3.28	15

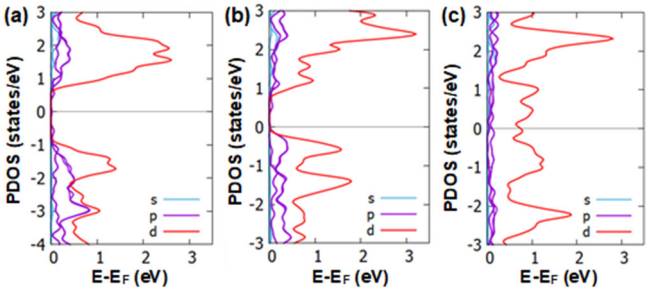

Fig 4. Calculated PDOS of (a) graphene/MoS_2, (b) graphene/$MoSe_2$, and (c) graphene/$MoTe_2$. Different color of plotting shows different orbital. Blue and purple represent the s and p orbital for C, S, Se and Te atoms, and red represents the d orbital for Mo atoms

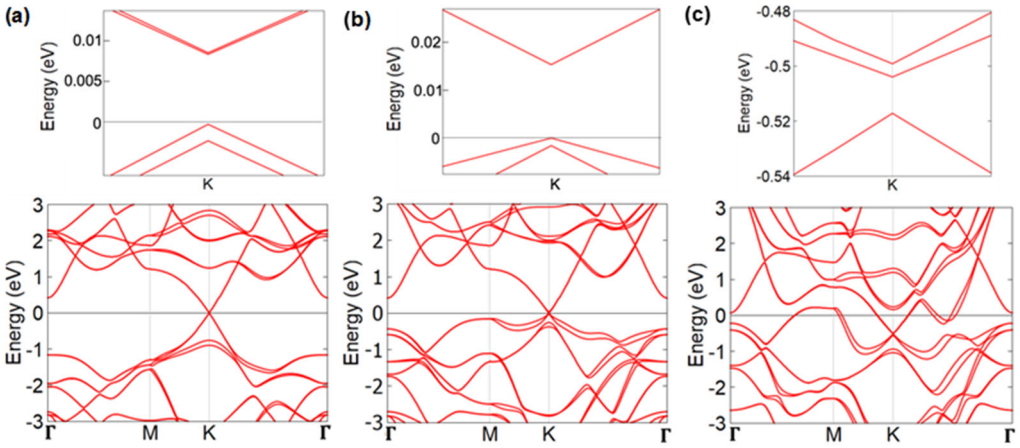

Fig 5. Calculated electronic structures of graphene/TMD heterostructures: (a) graphene/MoS_2, (b) graphene/$MoSe_2$, and (c) graphene/$MoTe_2$. Enlarged figures of Dirac bands are shown at the top of the figures. Zero energy sets to the top of the valence band in (a) and (b), and that in (c) sets to Fermi level

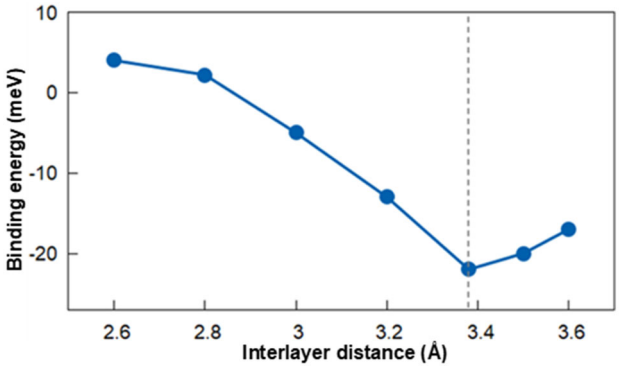

Fig 6. Binding energy (E_B) variation for 1:1 graphene/MoS_2 heterostructure concerning the interlayer distance. The dashed gray vertical line indicates the optimized interlayer distance with the lowest binding energy of -22 meV

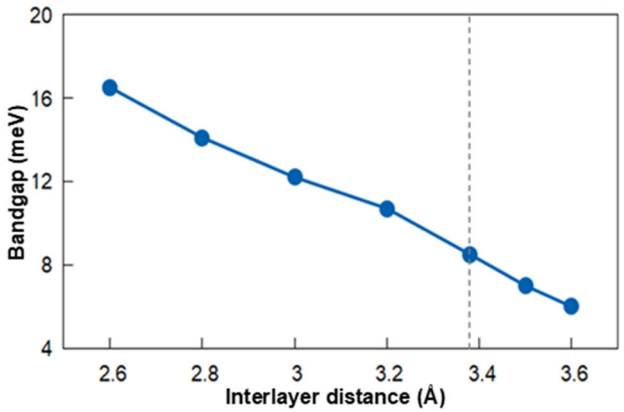

Fig 7. The calculated band gap of 1:1 graphene/MoS_2 heterostructure as a function of interlayer distance. The dashed grey vertical line portrays the optimized interlayer distance of the system at 3.38 Å with a band gap of 8.5 meV

Effect of Interlayer Distance

In a comprehensive analysis of interlayer distance, binding energy (E_B) between the graphene and MoS_2 layers was calculated by $E_B = E_{M/G} - (E_M + E_G)$, where $E_{M/G}$, E_M, and E_G are the total energies for the graphene/MoS_2, monolayer MoS_2, and monolayer graphene, respectively. The results are shown in Fig. 6. At an optimized interlayer distance of 3.38 Å, the calculated E_B reaches its lowest value of -22 meV, which corresponds with the previous work [46].

The dependence of interlayer distance on the bandgap at the K point in the graphene/MoS_2 is shown in Fig. 7, where the interlayer distance varies from 2.6 to 3.6 Å. As seen in the figure, at the optimum state of 3.38 Å of interlayer distance, the bandgap is 8.5 meV. The band gap is found to decrease when the interlayer distance increases gradually. Thus, widening interlayer distance between graphene and MoS_2 layers diminishes the orbital hybridization between the layers, leading to a pure graphene-like electronic structure with no bandgap.

■ CONCLUSION

We performed a first-principles calculation to investigate the effects of the electronic structures of graphene/MoS_2 heterostructure on stacking orientation, element substitution, and interlayer distance bonded through weak van der Waals interaction. We find that the electronic structures of graphene/MoS_2 are unlikely to be affected by stacking orientation. On the other hand, element substitution modifies the electronic properties, transforming the system to a metal characteristic. At last, the bandgap opening originating from the Dirac band in the graphene/MoS_2 may be tuned by the interlayer distance modification.

■ ACKNOWLEDGMENTS

This work is partly supported by Grants-in-Aid for Scientific Research (Grants numbers JP21K03444, JP21H04562, JP19K03716, and JP22K14290); the Tatematsu Foundation; the Okasan-Kato Foundation; the Research Foundation for the Electrotechnology of Chubu; the Data-Science Research Center for Material, Quantum, and Measurement Technologies, Mie University; and the Center for Spintronics Research Network, Osaka University. Numerical calculations were partially performed using computational facilities at Research Institute for Information Technology, Kyushu University and NIMS.

■ REFERENCES

[1] Novoselov, K.S., Geim, A.K., Morozov, S.V., Jiang, D., Katsnelson, M.I., Grigorieva, I.V., Dubonos, S.V., and Firsov, A.A., 2005, Two-dimensional gas of massless Dirac fermions in graphene, *Nature*, 438 (7065), 197–200.

[2] Novoselov, K.S., Geim, A.K., Morozov, S.V., Jiang, D., Zhang, Y., Dubonos, S.V., Grigorieva, I.V., and Firsov, A.A., 2004, Electric field effect in atomically thin carbon films, *Science*, 306 (5696), 666–669.

[3] Chung, C., Kim, Y.K., Shin, D., Ryoo, S.R., Hong, B.H., and Min, D.H., 2013, Biomedical applications of graphene and graphene oxide, *Acc. Chem. Res.*, 46 (10), 2211–2224.

[4] Zhang, W., Chuu, C.P., Huang, J.K., Chen, C.H., Tsai, M.L., Chang, Y.H., Liang, C.T., Chen, Y.Z., Chueh, Y.L., He, J.H., Chou, M.Y., and Li, L.J., 2015, Ultrahigh-gain photodetectors based on atomically thin graphene-MoS_2 heterostructures, *Sci. Rep.*, 4, 3826.

[5] Castro, E.V., Novoselov, K.S., Morozov, S.V., Peres, N.M.R., dos Santos, J.M.B.L., Nilsson, J., Guinea, F., Geim, A.K., and Castro Neto, A.H., 2007, Biased bilayer graphene: Semiconductor with a gap tunable by the electric field effect, *Phys. Rev. Lett.*, 99 (21), 216802.

[6] Avsar, A., Tan, J.Y., Taychatanapat, T., Balakrishnan, J., Koon, G.K.W., Yeo, Y., Lahiri, J., Carvalho, A., Rodin, A.S., O'Farrell, E.C.T., Eda, G., Castro Neto, A.H., and Özyilmaz, B., 2014, Spin-orbit proximity effect in graphene, *Nat. Commun.*, 5 (1), 4875.

[7] Fu, S., Wang, D., Ma, Z., Liu, G., Zhu, X., Yan, M., and Fu, Y., 2021, The first-principles study on the halogen-doped graphene/MoS_2 heterojunction, *Solid State Commun.*, 334-335, 114366.

[8] Tang, S., Wu, W., Xie, X., Li, X., and Gu, J., 2017, Band gap opening of bilayer graphene by graphene oxide support doping, *RSC Adv.*, 7 (16), 9862–9871.

[9] Tayyab, M., Hussain, A., Adil, W., Nabi, S., and Asif, Q.A., 2020, Band-gap engineering of graphene by Al doping and adsorption of Be and Br on impurity: A computational study, *Comput. Condens. Matter*, 23, e00463.

[10] Matis, B.R., Burgess, J.S., Bulat, F.A., Friedman, A.L., Houston, B.H., and Baldwin, J.W., 2012, Surface doping and band gap tunability in hydrogenated graphene, *ACS Nano*, 6 (1), 17–22.

[11] Hirahara, T., Ebisuoka, R., Oka, T., Nakasuga, T., Tajima, S., Watanabe, K., Taniguchi, T., and Yagi, R., 2018, Multilayer graphene shows intrinsic resistance peaks in the carrier density dependence, *Sci. Rep.*, 8 (1), 13992.

[12] Zhang, Y., Tang, T.T., Girit, C., Hao, Z., Martin, M.C., Zettl, A., Crommie, M.F., Shen, Y.R., and Wang, F., 2009, Direct observation of a widely tunable bandgap in bilayer graphene, *Nature*, 459 (7248), 820–823.

[13] Cao, X., Shi, J.J., Zhang, M., Jiang, X.H., Zhong, H.X., Huang, P., Ding, Y.M., and Wu, M., 2016, Band gap opening of graphene by forming heterojunctions with the 2D carbonitrides nitrogenated holey graphene, g-C_3N_4, and g-CN: Electric field effect, *J. Phys. Chem. C*, 120 (20), 11299–11305.

[14] Gmitra, M., and Fabian, J., 2017, Proximity effects in bilayer graphene on monolayer WSe_2: Field-effect spin valley locking, spin-orbit valve, and spin transistor, *Phys. Rev. Lett.*, 119 (14), 146401.

[15] Singh, S., Espejo, C., and Romero, A.H., 2018, Structural, electronic, vibrational, and elastic properties of graphene/MoS_2 bilayer heterostructures, *Phys. Rev. B*, 98 (15), 155309.

[16] Yu, X., Zhao, G., Gong, S., Liu, C., Wu, C., Lyu, P., Maurin, G., and Zhang, N., 2020, Design of MoS_2/Graphene van der Waals heterostructure as highly efficient and stable electrocatalyst for hydrogen evolution in acidic and alkaline media, *ACS Appl. Mater. Interfaces*, 12 (22), 24777–24785.

[17] Yin, Z., Li, H., Li, H., Jiang, L., Shi, Y., Sun, Y., Lu, G., Zhang, Q., Chen, X., and Zhang, H., 2012, Single-layer MoS_2 phototransistors, *ACS Nano*, 6 (1), 74–80.

[18] Lee, E., Yoon, Y.S., and Kim, D.J., 2018, Two-dimensional transition metal dichalcogenides and metal oxide hybrids for gas sensing, *ACS Sens.*, 3 (10), 2045–2060.

[19] Peng, Q., and De, S., 2013, Outstanding mechanical properties of monolayer MoS_2 and its application in elastic energy storage, *Phys. Chem. Chem. Phys.*, 15 (44), 19427–19437.

[20] Han, S.A., Bhatia, R., and Kim, S.W., 2015, Synthesis, properties and potential applications of

two-dimensional transition metal dichalcogenides, *Nano Convergence*, 2 (1), 17.

[21] Splendiani, A., Sun, L., Zhang, Y., Li, T., Kim, J., Chim, C.Y., Galli, G., and Wang, F., 2010, Emerging photoluminescence in monolayer MoS_2, *Nano Lett.*, 10 (4), 1271–1275.

[22] Zhang, Z.Y., Si, M.S., Wang, Y.H., Gao, X.P., Sung, D., Hong, S., and He, J., 2014, Indirect-direct band gap transition through electric tuning in bilayer MoS_2, *J. Chem. Phys.*, 140 (17), 174707.

[23] Nevalaita, J., and Koskinen, P., 2018, Atlas for the properties of elemental two-dimensional metals, *Phys. Rev. B*, 97 (3), 035411.

[24] Baik, S.S., Im, S., and Choi, H.J., 2017, Work function tuning in two-dimensional MoS_2 field-effect-transistors with graphene and titanium source-drain contacts, *Sci. Rep.*, 7 (1), 45546.

[25] Zhang, F., Li, W., Ma, Y., Tang, Y., and Dai, X., 2017, Tuning the Schottky contacts at the graphene/WS_2 interface by electric field, *RSC Adv.*, 7 (47), 29350–29356.

[26] Roy, K., Padmanabhan, M., Goswami, S., Sai, T.P., Ramalingam, G., Raghavan, S., and Ghosh, A., 2013, Graphene-MoS_2 hybrid structures for multifunctional photoresponsive memory devices, *Nat. Nanotechnol.*, 8 (11), 826–830.

[27] Han, S.W., Kwon, H., Kim, S.K., Ryu, S., Yun, W.S., Kim, D.H., Hwang, J.H., Kang, J.S., Baik, J., Shin, H.J., and Hong, S.C., 2011, Band-gap transition induced by interlayer van der Waals interaction in MoS_2, *Phys. Rev. B*, 84 (4), 045409.

[28] Gmitra, M., Kochan, D., Högl, P., and Fabian, J., 2016, Trivial and inverted Dirac bands and the emergence of quantum spin Hall states in graphene on transition-metal dichalcogenides, *Phys. Rev. B*, 93 (15), 155104.

[29] Lee, C.S., and Kim, T.H., 2021, Large-scale preparation of MoS_2/graphene composites for electrochemical detection of morin, *ACS Appl. Nano Mater.*, 4 (7), 6668–6677.

[30] Wen, X., Chen, H., Wu, T., Yu, Z., Yang, Q., Deng, J., Liu, Z., Guo, X., Guan, J., Zhang, X., Gong, Y., Yuan, J., Zhang, Z., Yi, C., Guo, X., Ajayan, P.M., Zhuang, W., Liu, Z., Lou, J., and Zheng, J., 2018, Ultrafast probes of electron-hole transitions between two atomic layers, *Nat. Commun.*, 9 (1), 1859.

[31] Liu, Y., Liu, C., Wang, X., He, L., Wan, X., Xu, Y., Shi, Y., Zhang, R., and Wang, F., 2018, Photoresponsivity of an all-semimetal heterostructure based on graphene and WTe_2, *Sci. Rep.*, 8 (1), 12840.

[32] Zhang, K., Fang, X., Wang, Y., Wan, Y., Song, Q., Zhai, W., Li, Y., Ran, G., Ye, Y., and Dai, L., 2017, Ultrasensitive near-infrared photodetectors based on a graphene-$MoTe_2$-graphene vertical van der Waals heterostructure, *ACS Appl. Mater. Interfaces*, 9 (6), 5392–5398.

[33] Gao, A., Liu, E., Long, M., Zhou, W., Wang, Y., Xia, T., Hu, W., Wang, B., and Miao, F., 2016, Gate-tunable rectification inversion and photovoltaic detection in graphene/WSe_2 heterostructures, *Appl. Phys. Lett.*, 108 (22), 223501.

[34] Akinwande, D., Petrone, N., and Hone, J., 2014, Two-dimensional flexible nanoelectronics, *Nat. Commun.*, 5 (1), 5678.

[35] Huo, N., Wei, Z., Meng, X., Kang, J., Wu, F., Li, S.S., Wei, S.H., and Li, J., 2015, Interlayer coupling and optoelectronic properties of ultrathin two-dimensional heterostructures based on graphene, MoS_2 and WS_2, *J. Mater. Chem. C*, 3 (21), 5467–5473.

[36] Wimmer, E., Krakauer, H., Weinert, M., and Freeman, A.J., 1981, Full-potential self-consistent linearized-augmented-plane-wave method for calculating the electronic structure of molecules and surfaces: O_2 molecule, *Phys. Rev. B*, 24 (2), 864.

[37] Weinert, M., Wimmer, E., and Freeman, A.J., 1982, Total-energy all-electron density functional method for bulk solids and surfaces, *Phys. Rev. B*, 26 (8), 4571–4578.

[38] Perdew, J.P., Burke, K., and Ernzerhof, M., 1996, Generalized gradient approximation made simple, *Phys. Rev. Lett.*, 77 (18), 3865–3868.

[39] Bučko, T., Hafner, J., Lebègue, S., and Ángyán, J.G., 2010, Improved description of the structure of molecular and layered crystals: Ab initio DFT

calculations with van der Waals corrections, *J. Phys. Chem. A*, 114 (43), 11814–11824.

[40] Nakamura, K., Ito, T., Freeman, A.J., Zhong, L., and Fernandez-de-Castro, J., 2003, Enhancement of magnetocrystalline anisotropy in ferromagnetic Fe films by intra-atomic noncollinear magnetism, *Phys. Rev. B*, 67 (1), 014420.

[41] Tao, P., Guo, H.H., Yang, T., and Zhang, Z.D., 2014, Stacking stability of MoS_2 bilayer: An ab initio study, *Chin. Phys. B*, 23 (10), 106801.

[42] Rasmussen, F.A., and Thygesen, K.S., 2015, Computational 2D materials database: Electronic structure of transition-metal dichalcogenides and oxides, *J. Phys. Chem. C*, 119 (23), 13169–13183.

[43] Sachs, B., Britnell, L., Wehling, T.O., Eckmann, A., Jalil, R., Belle, B.D., Lichtenstein, A.I., Katsnelson, M.I., and Novoselov, K.S., 2013, Doping mechanisms in graphene-MoS_2 hybrids, *Appl. Phys. Lett.*, 103 (25), 251607.

[44] Singh, A.K., Kumar, P., Late, D.J., Kumar, A., Patel, S., and Singh, J., 2018, 2D layered transition metal dichalcogenides (MoS_2): Synthesis, applications and theoretical aspects, *Appl. Mater. Today*, 13, 242–270.

[45] Ebnonnasir, A., Narayanan, B., Kodambaka, S., and Ciobanu, C.V., 2014, Tunable MoS_2 bandgap in MoS_2-graphene heterostructures, *Appl. Phys. Lett.*, 105 (3), 031603.

[46] Liu, B., Wu, L.J., Zhao, Y.Q., Wang, L.Z., and Cai, M.Q., 2016, First-principles investigation of the Schottky contact for the two-dimensional MoS_2 and graphene heterostructure, *RSC Adv.*, 6 (65), 60271–60276.